Available online at www.sciencedirect.com
SCIENCE DIRECT®

Journal of the European Ceramic Society 24 (2004) 2619–2629
www.elsevier.com/locate/jeurceramsoc

Formation, sintering and thermal expansion behaviour of Sr- and Mg-doped $LaCrO_3$ as SOFC interconnector prepared by the ethylene glycol polymerized complex solution synthesis method

P. Duran*, J. Tartaj, F. Capel, C. Moure

Instituto de Cerámica y Vidrio (CSIC) Camino de Valdelatas, s/n, Campus de Cantoblanco, 28049, Madrid, Spain

Received 16 July 2003; received in revised form 15 September 2003; accepted 20 September 2003

Abstract

Sr- and Mg-doped $LaCrO_3$ nanosized powders were succesfully synthesized from a polymeric precursor solution containing the respective aqueous solution of metal nitrate, chromium (III) nitrate, nitric acid, and ethylene glycol. The presence of a chromate solid solution of the type $La_{0.8}Sr_{0.2}Cr_{1-x}Mg_xO_4$ ($x \leqslant 0.2$) as a low-temperature intermediate to perovskite-type is experimentally established using TG/DTA and XRD. In Sr, Mg-substituted $LaCrO_3$, single-phase perovskite $La_{0.8}Sr_{0.2}Cr_{1-x}Mg_xO_3$ was formed at about 770 °C by decomposition of the chromate phase solid solution, which crystallizes at about 520 °C from amorphous powders. $La_{0.8}Sr_{0.2}Cr_{1-x}Mg_xO_3$ perovskite solid solution powders with surface areas as high as 11 m^2/g and nanosized particles sintered at 1550 °C for 6 h in air were higher than 97% dense materials. Such an improvement in densification can be attributed to a two-stage shrinkage process, i.e., liquid phase formation and solid perovskite particle rearrangement in the liquid, respectively. No significant variations in both the final density and grain size with increasing Mg content were detected. Compositions $La_{0.8}Sr_{0.2}Cr_{0.9}Mg_{0.1}O_3$ and $La_{0.8}Sr_{0.2}Cr_{0.85}Mg_{0.15}O_3$ here investigated were shown to have negligible thermal expansion mismatch with YSZ electrolytes. The mixed oxide route was also used for comparison.

Keywords: (La, Sr)CrO_3; Fuel cells; Interconnect; Precursors-organic; Sintering; Thermal expansion

1. Introduction

Because of its high electronic conductivity and its superior thermal stability, lanthanum chromite doped with several percentages of Mg,Ca, and Sr oxides is being currently used as the interconnecting material in the planar model SOFC's.[1,2] It has been well established that the substitution of either on A or B sites in the ABO_3 perovskite materials with acceptor or donor-type cations may improve the electrical properties.[3,4] Furthermore, the thermal expansion of this compound matches very well with that of YSZ electrolyte.[5]

Although thermal-electrical properties of the alkaline-earth-doped lanthanum chromites become this material as the most promising candidate for SOFC device interconnectors,[6] its sinterability, which is another requirement, is very bad in air due to the high vapor pressure of the chromium oxide.[7] Therefore, a good powder preparation method, in order to achieve more reactive and sinterable powders, becomes necessary. Many attempts leading to achieve doped-lanthanum chromite sinterable powders have been carried out. Among them, mainly two have attracted the attention of the researchers, (a) the Pechini method also called "liquid mix", and (b) the combustion reaction method. Both make use of liquid solutions of the desired metal ions leading to the final oxide powders. The advantages and disadvantages of these methods have been widely studied by several authors.[8–10] Briefly, the first one is based on the chelation of complex cations leading to the formation of an intermediate resin, which, on charring and calcining, leads to a sinterable powder. In the second one, which is essentially based on that of self-propagating high temperature synthesis makes use of a fuel (usually urea) to produce a spontaneous flame with no controlled temperature (>1200 °C) leading in a short

* Corresponding author. Tel.: +34-91-735-5854; fax: +34-91-735-5843.
E-mail address: pduran@icv.csic.es (P. Duran).

0955-2219/$ - see front matter © 2003 Elsevier Ltd. All rights reserved.
doi:10.1016/j.jeurceramsoc.2003.09.016

time to a foamy but well crystallized single-phase powder. This uncontrolled synthesis temperature may be the cause for obtaining relatively poor sinterable powders.[11–13]

Although the objective of the above mentioned wet-chemical methods was to achieve more reactive perovskite powders at a temperature as low as possible, the truth is that in the majority of the cases the sintering of the obtained powders has to be made at temperatures in the range of 1400–1700 °C for densification levels in the range of 92–95% of theoretical density. The use of reducing atmospheres, substitution of chromium by other transition metals, or the addition of sintering aids have been some of the chosen processing ways for improving their sinterability.[7,14–17] Although in the last decade the initial assumption of the cosintering of the several cell components has been changed for that of the electrolyte-supported strategy, a low-temperature sintering is desirable in order to avoid chemical reactions with the other components of the fuel cell. Therefore, it becomes necessary to investigate new chemical synthesis methods leading to achieve low-temperature sinterability perovskite powders. In the present study, the synthesis and characterization of mainly $La_{.0.8}Sr_{0.2}Cr_{0.8}$ $Mg_{0.2}$ perovskite referred to throughout as EG–LSCM powders, at relatively low-temperature, is described using the ethylene glycol process..[18] The reaction mechanism of the precursors leading to the perovskite single-phase, and the powder processing for making dense chromite bodies are discussed. For comparison, the same composition referred to throughout as MO–LSCM powders using the mixed oxides route, was prepared.

2. Experimental procedure

Lanthanum chromite powders, basically $La_{0\cdot8}Sr_{0\cdot2}Cr_{0.8}$ $Mg_{02}O_3$ were prepared by the soft solution process. Lanthanum nitrate ($La(NO_3)_3.6H_2O$,99.99% pure), Strontium nitrate $Sr(NO_3)_2.4H_2O$,99.9% pure), chromium nitrate ($Cr(NO_3)_3.9H_2O$,99.9% pure), magnesium acetate ($Mg(CH_3–COO)_2.4H_2O$,99.9% pure), nitric acid (HNO_3,65%),and ethylene glycol ($HOCH_2–CH_2OH$,99.9% pure) were used as starting raw materials. Fig. 1 shows the preparation flow chart. Aqueous solutions of all of them were adjusted in the required amounts by dissolving in distilled water and mixed altogether in nitric acid to form a solution by stirring. To this transparent solution was added dropwise ethylene glycol in equivalent molar proportion to the amount of the metal cation present, by stirring. The as prepared transparent solution was then heated on a hot plate at about 60–80 °C with magnetic stirring until a gel was obtained. The polymerized gel was dried at 130 °C in an oven for several hours forming a resin and, finally, the dried resin

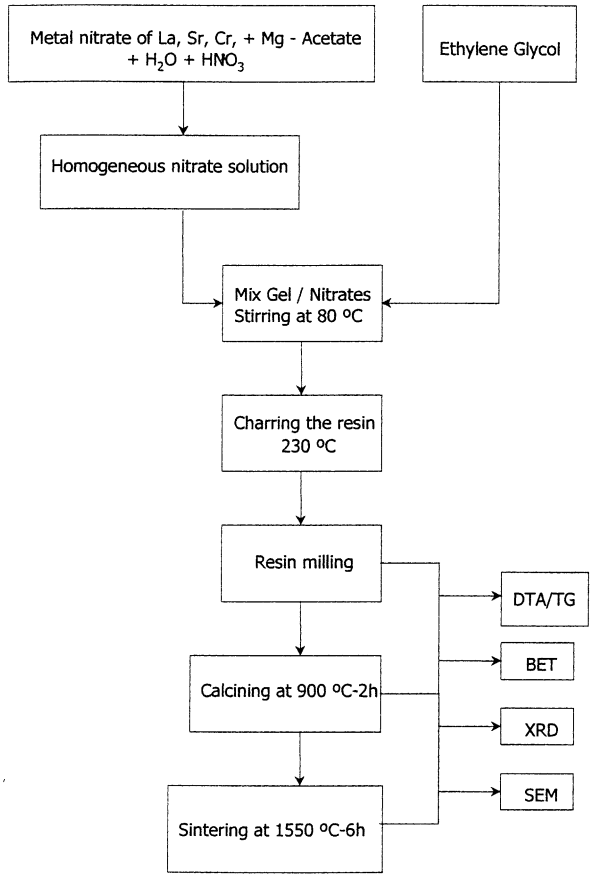

Fig. 1. Flow chart of synthesis and characterization of the EG–LSCM powders from polymerized complex solution.

was heat-treated at 230 °C. The decomposition and reaction processes were examined with a DTA/TG thermal analyzer (Model STA 409, Netzsch) in air with a heating rate of 10 °C/min from room temperature to 900 °C. α-Alumina was used as the reference in DTA. Furthermore, the calcination treatments of the dried resin were carried out at 230–900 °C for 4 h in air to study the phase transformations, crystallization, and sinterability of the obtained powders. The as prepared powders were examined by X-ray diffraction (XRD) with a goniometer scanning speed of 2° 2θ/min Lattice parameters of the sintered samples were obtained in the 20–75 2θ range using Cu $K\alpha$ radiation (0.154060 nm). Lattice parameters were calculated for single-phase solid solution $La_{0.8}Sr_{0.2}Cr_{1-x}Mg_x$ O_3 ($0 \leqslant x \leqslant 0.20$). The procedure involved mixing the powders with a silicon standard followed by slow scanning through the orthorhombic 440, 008, 044, and 404 hkl reflections at step intervals of 0.01° 2θ, with a 4 s time constant. The scan range was chosen to include a Si reflection so that the error in 2θ could be corrected. Powders were observed by scanning electron microscopy (SEM, model DSM 950,Karl Zeiss, Inc., Oberkochem, Germany). The BET specific surface areas of the calcined powders

were measured with the Quantachrome Autosorb (Model MS-16, Quantachrome Corp., Suoset, NY).

Before sintering, calcined powders were attrition milled for 2 h in methanol with zirconia ball media. After drying, the powders were granulated and isopressed into pellets at 200 MPa. In order to avoid the grain growth in the low temperature region, the temperature was firstly raised at a heating rate of 5 °C/min up to 700 °C for a few minutes, and from this point a heating rate of 20 °C/min was used if not otherwise stated up to the sintering temperature of 1550 °C. The holding time was in all cases 6 h at the higher sintering temperature. In order to study the evolution in microstructure, the green compacts were also sintered at a constant heating rate of 2 °C/min at 1200 to 1500 °C for 2h in air, with a dilatometer (Model 402E/7, Netzsch, Germany). After sintering, bulk densities of the sintered samples were measured by the Archimedes method, the pore-distribution was studied mercury porosimetry, (Micromeritics, Autopore II, 9215, Norgross, USA), and microstructural observations on the surface of the fractured or polished samples were carried out by SEM. The average grain size was measured by the interception method. Thermal expansion coefficient (TEC) of the different EG–LSCM perovskite samples was measured using the above mentioned dilatometer equipment in the temperature range from 50 to 1000 °C. The measurement in air was performed using a heating rate of 5 °C/min, and the TECs of the perovskite samples were calculated from the following equation:

$$\alpha = (1/L_1)(L_2 - L_1)(T_2 - T_1)$$

Where α is the TEC, T_1 is the starting temperature, T_2 is the final temperature, and L_1 and L_2 are the initial and final lengths, respectively.

3. Experimental results

3.1. Synthesis of $La_{08}Sr_{02}Cr_{1\text{-}x}Mg_x$ O_3 perovskite phase

Fig. 2 shows the DTA/TG curve of the resin powder previously charred at 230 °C for several hours in the case of the $La_{0.8}Sr_{0.2}Cr_{0.8}Mg_{0.2}$ O_3 composition. Similar DTA/TG curves for the other $La_{0.8}Sr_{0.2}Cr_{1-x}Mg_x$ O_3 perovskite compositions were registered and, therefore, they will not be reported here. A small endothermic peak up to 150 °C is present as a consequence of the loss of the residual adsorbed and hydrated water with a weight loss of about 2%. From 150 °C up to about 500 °C a strong and wide exothermic effect with a weight loss of about 23% also is present in the DTA curve. Such an exothermic effect is associated with the decomposition–oxidation of the metal-chelates and the evolved gases, and reaction of the decomposed chelates.

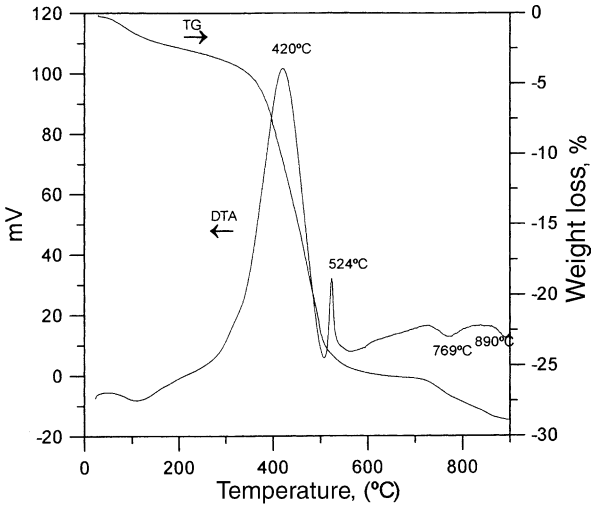

Fig. 2. DTA/TG curves of the solid intermediates from the polymerized complex EG–LSCM precursor solutions with heating rate of 10 °C/min.

As a consequence of the reaction in the decomposed metal-chelates, the DTA curve shows at 525 °C a second exothermic peak, which corresponds to the crystallization of a complex oxide byproducts. The fact that no weight loss accompanies this exothermic effect supports the above statement. As we will describe below, this exothermic peak was found to result from the crystallization of a chromate phase $La_{0.8}Sr_{0.2}Cr_{0\cdot8}Mg_{0.2}$ O_4 solid solution. In addition to this, the DTA curve revealed another two small endothermic peaks at 769 and 890 °C with a weight loss of about 4% in the TG curve. This last weight loss can be associated, in principle, with the decomposition of the chromate phase to give the chromite one by releasing oxygen i.e., $La_{0.8}Sr_{0.2}Cr_{0.8}Mg_{0.2}O_4 \longrightarrow La_{0.8}Sr_{0.2}Cr_{0.8}Mg_{0.2}O_3 + 1/2O_2$.

To further support such a belief a part of the resin charred at 230 °C was attrition-milled with isopropyl alcohol for 2 h and calcined at 550 °C for 16 h in air. The as obtained powders greenish in color were almost a chromate $La_{0.8}Sr_{0.2}Cr_{0.8}Mg_{0.2}O_4$ single phase. Fig. 3 shows the evolution of the structure studied by XRD between 230 and 1400 °C. As it can be observed the amorphous resin decomposes above 300 °C leading to the rapid appearance of the $La_{0.8}$ $Sr_{0.2}$ Cr_xMg_{1-x} O_4 not completely formed chromate phase solid solution. The presence of a certain amount of amorphous material at 500 °C indicates that the reaction for the formation of the chromate phase was not yet completed. Free oxides or other secondary phases were not detected at this temperature. At 600 °C for 2 h, a well-crystallized chromate phase was formed as the only intermediate before the formation of the chromite phase. All X-ray diffraction lines for this sample are similar to those of $LaCrO_4$,[19] and could be indexed as a monoclinic unit

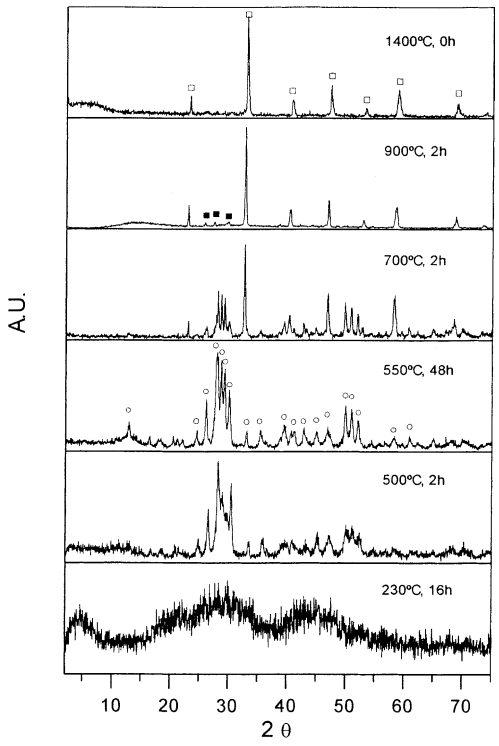

Fig. 3. XRD patterns of the solid intermediates from the polymerized complex EG–LSCM precursor solutions heated at the indicated temperatures.

cell with $a=0.7024$, $b=0.7251$, $c=0.6641\pm0.0005$ nm, and $\beta=104.39°$, agreeing well with crystallographic data $a=0.7041$, $b=0.7237$, $c=0.6693$ nm, and $\beta=104.94°$.[19] The small differences found in the lattice parameters are due to the fact that the present compound is not a pure lanthanum chromate but a chromate phase solid solution.

According to our X-ray studies the chromate phase becomes unstable at temperatures above 700 °C and transforms to perovskite-type phase by releasing oxygen. At this point a color change from greenish to brown in the powder sample took place, which evidenced a transformation in the crystal structure, with the change in the coordination number for the La and Cr atoms.[19] X-ray analysis on powders calcined at 900 °C for 2 h and slowly cooled indicated the formation of a clear perovskite phase solid solution. In addition to such a perovskite phase, a minoritary second phase always was present, and it seems to correspond to a residual $SrCrO_4$ phase.[20] The appearance of X-ray reflections at $2\theta=25.84$ (62), 27.45(100), and 29.84(94) (in parentheses: the relative peak intensity), support the above contention. It is indicating that during calcination a part of the Sr is exsoluted from the perovskite structure forming the chromate phase and other no detected minor phases. X-ray diffraction analysis on a sintered sample at 1400 °C showed that the strontium chromate phase had been decomposed and dissolved into the perovskite phase matrix. The lattice parameters of the chromite single-phase solid solution were, $a=0.5487$, $b=0.7770$ and $c=0.5483\pm0.0003$ nm according to an orthorhombic symmetry ($Z=4$ and Pnma space group). It must be mentioned that in the case of the mixed oxides route, the chromite phase only was obtained after prolonged heat-treatments (>10 h) at 900 °C or higher temperatures. The lattice parameters for the $La_{0.8}Sr_{0.2}$ $Cr_{1-x}Mg_x$ O_3 perovskite phase increased lineraly with the Mg content and,therefore, the volume of the unit cells too as it will be seen below.

3.2. Powder morphology and characterization

Fig. 4 (A) and (B) shows the SEM micrographs of the two EG- and MO-LSCM calcined powder samples. EG powders after calcining at 900 °C for 2 h were an agglomerated one which consisted of submicron crystallites (0.2–0.6 μm). The agglomerates have a bimodal Gauss distribution with an average agglomerate size obtained using a laser diffraction particle analyzer of 0.9 μm. The BET specific surface area was in all the EG–LSCM compositions in the range of 10–11 m^2/g. The MO–LSCM powders showed a more uniform Gauss distribution curve but with a slightly higher average particle size of 1.2 μm; the BET specific surface area was about 6 m^2/g.

3.3. Sintering and microstructure development

The calcined LSCM powders, after isopressing at 200 MPa (compacts green density of about 50% theoretical density) showed a bimodal pore size distribution, not shown here, with two peaks centered at 20 and 90 nm in the case of the EG green compacts. In the case of the MO green compacts, only one peak in the pore size distribution curve centered at about l40 nm was registered. Both kinds of samples were sintered between room temperature and 1550 °C. The relative densities were estimated taking into account the theoretical density value of 6.28 g/cm^3 for the perovskite phase. This was calculated from molecular weights, the number of chemical formula units per unit cell ($Z=4$), Avogadro's number, and lattice parameters. Fig. 5 (A) shows the relative density of the LSCM samples sintered in air as a function of sintering temperature with no holding time. The density of both kinds of samples gradually increased with increasing temperature. The densification started at approximately the same temperature (about l100 °C) for the two kinds of samples, but the polymerized complex solution synthesis prepared samples showed better sintering characteristics. Thus, it is clear from the above figure that two sintering steps can be identified, the first one with maximum shrinkage rate at about 1200 °C, and the second one at 1420 °C. In the

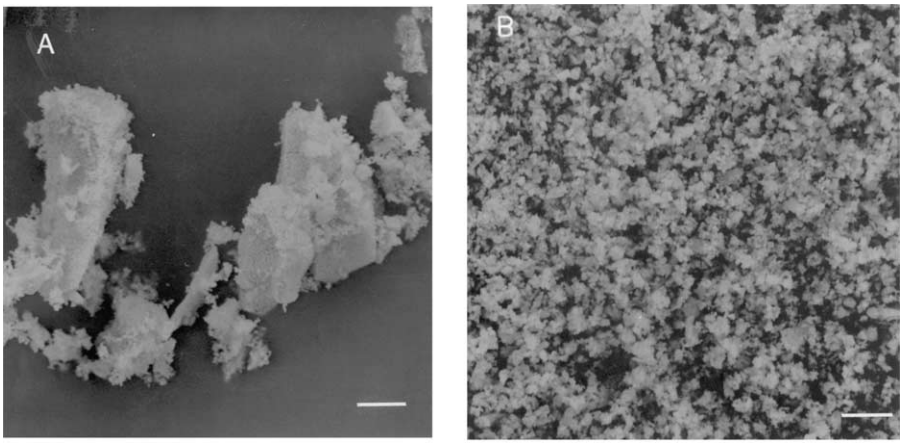

Fig. 4. SEM micrographs of (A) EG–LSCM and (B) MO–LSCM calcined powders (bar = 5 μm).

case of the samples prepared by the mixed oxide route, the same two sintering steps are present but displaced towards higher temperatures, i.e., at 1270 °C and above 1550 °C, respectively. It is also clear that the densification process takes place mainly between 1400 and 1600 °C. In that way, a study of the densification as function of the holding time was carried out at 1550 °C. The relative density, as shown in Fig. 5 (B), increased with increasing holding time and the main densification took place in the 0–6 h holding time range. Above that holding time the density value was almost constant or decreased. Therefore, it can be assumed a no effective influence of longer heat-treatment on sintering. A maximum density value of 97% of theoretical density was obtained for the polymerized complex solution prepared samples after sintering at 1550 °C for 6 h,and only a 91% was achieved in the case of the mixed oxide prepared samples sintered in the same conditions. It must be mentioned that a small weight loss (about 1%) in the samples after sintering, was detected.

Fig. 6 (A)–(F) shows the micrographs of fracture surfaces of the $La_{0.8}Sr_{0.2}Cr_{0.8}Mg_{0.2}$ O_3 samples sintered at 1200 to 1600 °C for 2 h. Apparently, almost no grain growth took place at this temperature interval, since the grain size was about 0.3 μm at the lower sintering temperature and about 0.5 μm at the higher sintering one, and a similar tendency with increasing Mg content was found. A small amount of liquid like a whisker can be observed at 1400 °C, Fig. 6 (D). Fig. 7 (A)–(C) are images of fracture surfaces of EG-LSCM (97% dense) and polished surfaces of MO–LSCM (91% dense) samples which were sintered at 1550 °C for 6 h. The grain sizes of EG–LSCM perovskite samples were relatively uniform and the aspect of the ceramic material with sharp grain corners is like a strong body in comparison to that of the MO–LSCM perovskite samples which appeared softer, Figs. 7 (A) and (B). No second phases were detected on the fracture surface of the EG–LSCM samples. Fig. 7 (C) shows a dark second phase observed between the perovskite grains of the MO–LSCM samples. According to the study by EDX, not shown here, the composition of this second phase mainly contained magnesium, with lanthanum and chromium in minor amounts. This is, likely, the result of a non uniform distribution of the different components in the prepared powder or, likely, we are near to the limit of the MgO solid solubility.

3.4. Thermal expansion coefficients

The ideal interconnect material for a SOFC device should have, among other relevant characterisitics, well-matched thermal expansion coefficient (TEC) with that of the other cell components. As mentioned above, several doped-lanthanum chromites on A and/or B perovskite sites have been proposed as good interconnector materials for SOFCs, but many of them have also been rejected because of their inadequate properties to fulfill the requirements for such an application. In the present case, we studied the combined effect of Sr^{2+} substitution in A sites and Mg^{2+} substitution in B sites of the perovskite structure, on the thermal expansion coefficients of the several lanthanum chromite materials comparatively with those of the others doped lanthanum chromites and that of the YSZ electrolyte. Table 1 shows the thermal expansion coefficients (TECs) of $La_{0.8}$ $Sr_{0.2}$ Cr_{1-x} Mg_x ($x \leqslant 0.2$) in air, and the calculated unit cell volumes. As is evident, doping with Mg^{2+} leads to a larger TEC of the sintered samples. In the same way, it has been observed that the structure of the samples was a slightly distorted orthorhombic with increasing Mg^{2+} content and, parallelly, an almost linear increase in the volume of the unit cell occurred. It must be noted that the cell volume of the 20 mol% MgO composition is slightly higher than that of the composition containing 15 mol% MgO. The TEC of the YSZ

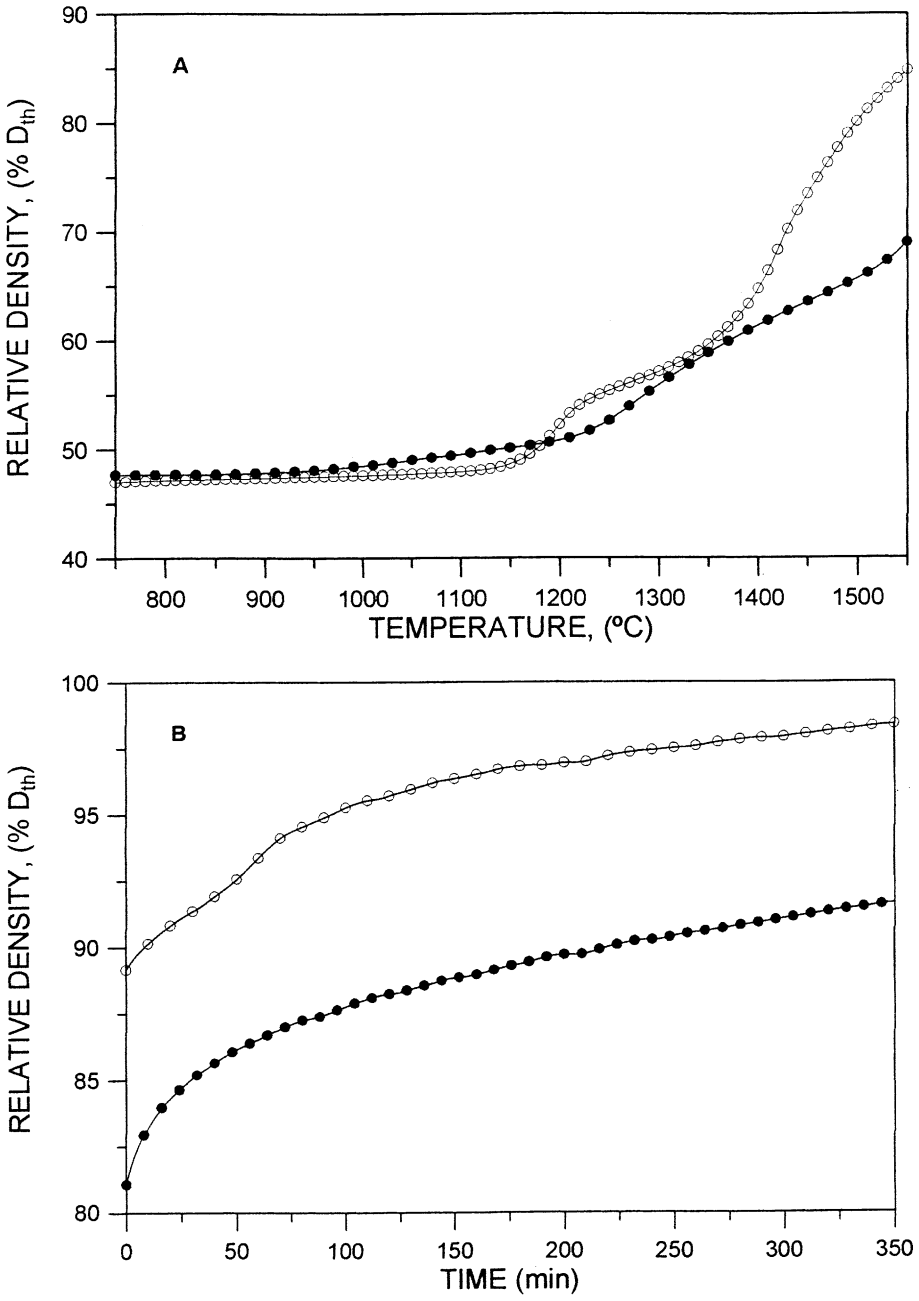

Fig. 5. Relative density of the EG-LSCM (open circles) and MO–LSCM (solid circles) as a function of (A) sintering temperature and (B) holding time at 1550 °C in air.

electrolyte material is between 9.9 and 10.6×10^{-6} °C^{-1} in the temperature range from room temperature (25 °C) to operating temperature (1000 °C). In the present work, for a constant concentration of SrO (20 mol%), the thermal expansion coefficients increased with increasing MgO content from 10 to 12×10^{-6}°C^{-1} for 10 and 20 mol% MgO, respectively. Undoped $LaCrO_3$ shows an orthorhombic to rhombohedral phase transformation at about 280 °C, but in the present case the phase transformation was not present in our samples indicating, thus, the benefit of the combined effect of Sr^{2+} and Mg^{2+} at the A and B sites, respectively.

4. Discussion

The preparation of LSCM perovskite powders by the mixed oxide route method needs quite longer annealing times and higher temperatures than the polymerized complex solution synthesis method. These results can be supported by much shorter diffusion distances in the case of the soft solution amorphous precursor powders, which can be due to the smaller particle size.

From the described experimental results, see Fig. 2, it seems to be that the first compound, as the only intermediate, that is formed during the perovskite phase

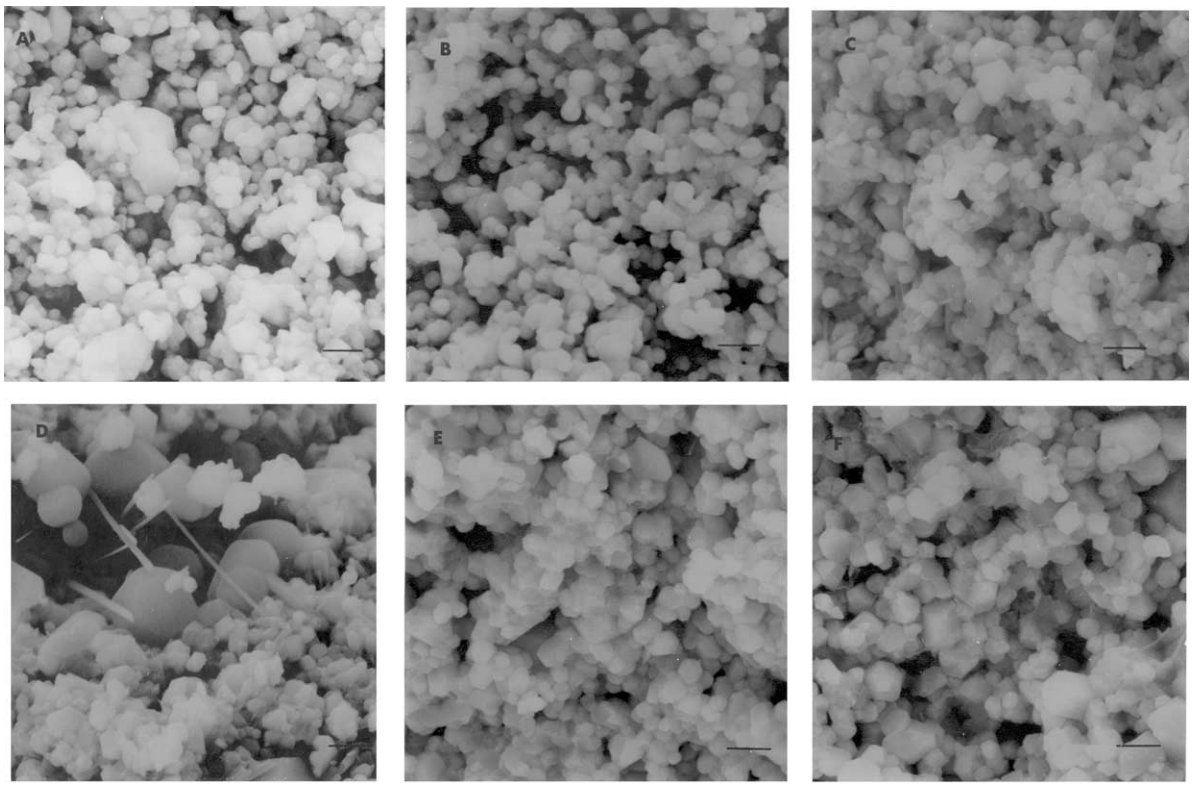

Fig. 6. SEM photomicrographs of fractured surfaces of EG–LSCM samples from sintering temperatures of (A) 1200, (B) 1300, (C) 1400, (E) 1500 and (F) 1600 °C for 2 h. (bar = 1 μm) and (D) 1400 °C for 2 h showing liquid phase like a whisker (bar = 0.5 μm).

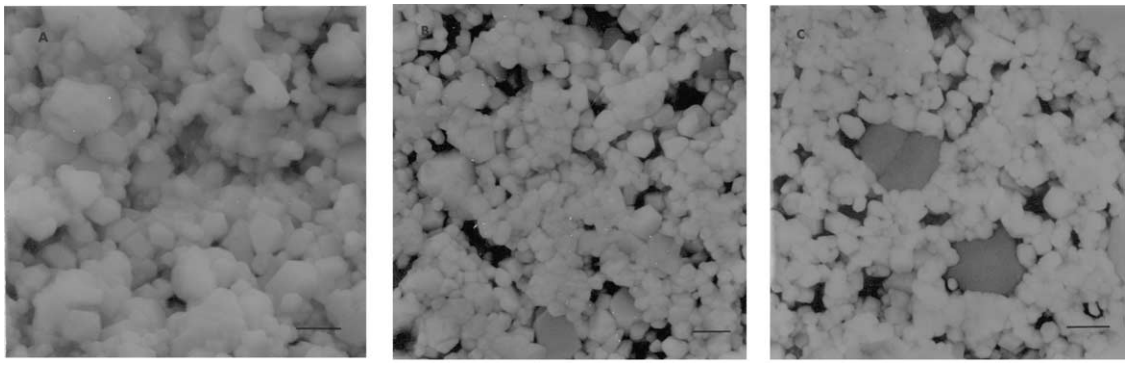

Fig. 7. SEM photomicrographs of (A) fractured surfaces of EG–LSCM and (B) polished and thermally etched surfaces of MO–LSCM samples sintered at 1550 °C for 6 h. In (C) the appearance of a dark second phase in MO–LSCM sintered samples is observed (bar = 1 μm).

Table 1
Cell volume and thermal expansion coefficients of undoped and Sr and Mg-doped lanthanum chromites

Samples	Cell volume (Å^3)	TEC ($\times 10^{-6}$/°C)
La Cr O_3	234.40	8.70
$La_{0.8}Sr_{0.2}CrO_3$	233.70	8.92
$La_{0.8}Sr_{0.2}Cr_{0.9}Mg_{0.1}O_3$	233.80	10.00
$La_{0.8}Sr_{0.2}Cr_{0.85}Mg_{0.15}O_3$	233.87	11.02
$La_{0.8}Sr_{0.2}Cr_{0.8}Mg_{0.2}O_3$	233.88	12.10
YSZ	NM[a]	10.60
$La_{0.8}Sr_{0.2}Cr_{0.9}Ti_{0.1}O_3$[37]	347.65	10.40
$La_{0.9}Sr_{0.1}Cr_{0.95}Co_{0.05}O_3$[28]	348.07	11.40

[a] No measured.

reaction synthesis is the $La_{0.8}Sr_{0.2}$ Cr_{1-x} Mg_xO_4 chromate phase solid solution, and this compound starts to form already at temperatures as low as 400 °C. The completion of such reaction formation takes place at about 550 °C coinciding with the end of the crystallization peak of the chromate phase solid solution. Such a chromate phase is transformed, between 720 and 830 °C; into the chromite phase La $_{0.8}$Sr $_{0.2}$$Cr_{1-x}$ Mg_x O_3 by releasing oxygen. Carter et al.,[19] using the Pechini method of synthesis, reported that when the (La,Ca)CrO_4 chromate phase was heated at about 700 °C, other intermediate products such as $LaCrO_3$ and $CaCrO_4$ were formed, and these two byproducts

subsequently combined to give the final (La,Ca) CrO_3 chromite solid solution. In the present work, above that transformation temperature the only present phase was the chromite solid solution which, on cooling, was accompanied by about 3–4% of a secondary phase identified as the strontium chromate ($SrCrO_4$), confirming the suggestions of Berg et al.[20] Such a secondary phase only disappeared after sintering at or above 1400 °C, see Fig. 3. This result supported the idea for an increase in the solid solubility of the strontium oxide in the chromite structure as the temperature increased.

Since the interconnect in the SOFC device must be gas-tight, the densification level of the perovskite material is of crucial importance. In the present work it has been demonstrated that when using the soft solution synthesis as the method for making dense bodies of doped-lanthanum chromite, the sintering in air is enhanced with respect to the mixed oxide route, see Fig. 5 (A). Two factors have to be considered as favorable in enhancing the sintering characteristics, (1) the smaller particle size of the as prepared powders, and (2) the doping to the A and B-sites with Sr^{2+} and Mg^{2+} cations. As a consequence, the sintering curves for the soft solution prepared powders are sifted to lower temperatures. A similar effect was reported for the case of Sr^{2+} doping to the A-site on perovskite material sintering.[21]

Given that the Sr^{2+} is exsoluted during calcination as $SrCrO_4$ and other derivatives, the global sintering process exhibits different steps, which could correspond to the melting of the formed compounds. In this maner, the shrinkage rate curve showed two pronounced inflections at about 1200 and 1420 °C. These two temperatures are lower than those reported when the perovskite samples were doped only with Sr^{2+}, 1250 and 1451 °C, respectively.[21] The first one can be ascribed to the melting of chromate phase.[22] In the absence of any other compound in the present sintered samples, the second inflection in the shrinkage rate curve can be due to a rapid rearrangement of the perovskite particles in the liquid with the elimination of pores via viscous flow at grain boundaries. Therefore, the two-steps densification behavior of these Sr- and Mg-doped lanthanum chromite samples can be considered as a liquid-phase assisted sintering.[23] The final relative density was as high as 97% of theoretical, which is much higher than that reported for others.[19,21] Therefore, the importance of Mg doping on B-site in enhancing densification of the perovskite samples should also be taken into account. In such a way, it has also been reported that a remarkable difference of sintering characteristics was observed for the Co-doped lanthanum chromites.[24] Quite recently, Mori et al.[25–27] have studied the possibilities for fully dense doped-lanthanum chromites taking into account the characteristics of the powders synthesized by the Pechini method,[28] comparing them with those prepared by both the solid state route and with the B-site doping. Their results, obtained on samples sintered at 1600 °C for 20 h, were moderately enhanced by B-site doping with Ni and V in which relative density only was raised up to about 90% theoretically. Powder synthesized by the solid state route were poorly densified in the same conditions .In agreement with the Mori et al.[28] results, it has been found that the B-site doping in the perovskite with Mg^{2+} improved sintering characteristics of the LSCM samples. It is probably due to both a decreasing in the formation temperature of liquid phase and an increasing in the amount of the liquid. It must be taken into account that the temperature of treatment with increasing holding time, 1550 °C, was located within the zone of higher shrinkage rate, and such a temperature could also be located, according to the SrO–chromium oxide phase diagram,[22] within the zone of the full formation of liquid phase as previously reported for the case of the V- or Ni-doped lanthanum chromite samples.[29,30] In that way, the increase of the relative density with increasing holding time, 97% of theoretical at 1550 °C for 6 h, would be favored, see Fig. 5 (B). Such a density value is much higher that that reported as acceptable (94% dense) for ceramic SOFC interconnector.[17]

As shown in Fig. 5, substituting 20 mol% strontium and magnesium onto A and B-sites, respectively, in the perovskite structure results in two distinct regions of densification behavior. The first region commences at around ll50 °C and continues up to about l220 °C where there is an inflection in the densification curve suggesting a change in the sintering mechanism of the sample. A density change of about 12% took place in the sample at this temperature interval. The transient liquid phase which relatively improves densification of the sample is likely to have been formed by the incongruent melting of $SrCrO_4$ present in the calcined powders to a strontium oxychromate liquid with general formula $Sr_m(CrO_4)_n$, where $m > n$, which changes in composition with temperature.[22] The low densification achieved at this first inflection can be related to the high viscosity of the formed liquid and only the smaller pores are eliminated, i.e., the formed liquid phase seems to be not very effective for densification.

A plausible explanation for such behavior would be as follows. Given that the particle size of soft solution prepared samples is on the nanoscale, a relatively strong capillary pressure and rapid rearrangement of the solid particles in the generated liquid by the melting of the $SrCrO_4$, develops as the driving force for the high shrinkage rate at this sintering temperature but with a relatively high densification. If the perovskite grains are surrounded and wetted by the liquid phase, a capillary force from such a wetting liquid combined with small transport distances should contribute to a rapid densifi-

cation with increasing temperature. However, this did not occurr at this sintering temperature, i.e., relevant densification was never attained at this first sintering step. With increasing temperature and sufficient amount of liquid phase, a decrease in the viscosity and homogenization of the liquid occurs as a consequence of the capillary forces. Given that the sintering process is dominated by the elimination of pores, then in the second sintering step a pore-filling process takes place with both a rapid pore elimination via a viscous-flow mechanism and a strong shrinkage rate. In fact, the dilatometric experiments, see Fig. 5, showed a high densification up to 1550 °C, which is due to the rapid rearrangement of the small perovskite particles in the generated liquid with almost no grain growth, see Fig. 6. This small grain growth can be explained by a low dissolution rate of the perovskite particles in the formed liquid. Although such a statement would be contradictory to the conventionally assumed solution-precipitation mechanism,[31] it seems evident that a steady-state Ostwald ripening mechanism for the grain-growth did not occur. On the other hand, it can be argued that the volume fraction of the generated liquid was small (as a consequence of the relatively small amount of the present $SrCrO_4$ phase), and the average liquid layer, if any, surrounding the perovskite particles will be very thin. The lack of achievement of dense perovskite bodies at the end of the sintering process is, likely, supporting the above contentions. However, it is suggested that more efforts should be made to reach a better knowledge on the sintering of these ceramic materials.

Summarizing from the above, it can be stated that the sintering of the LSCM perovskite samples takes place in two well-established steps. At the first sintering step the formed liquid phase was ineffective in improving densification. In fact a limited shrinkage occurs at the beginning of sintering, see Fig. 5. This result would confirm the idea reported by Sakai et al.[23] which attributed this first sintering step only to a particle rearrangement with no liquid formation. But if the existence of $SrCrO_4$ as a minor second phase in the calcined powders is taken into account, it should be assumed that the formation of a small amount of liquid in which a certain rearrangement of the smaller perovskite particles takes place with a low densification. On the other hand, the small grain growth observed at this sintering step would be in agreement with such a statement. Furthermore, it was found on the cooled samples from this sintering step the absence of any $SrCrO_4$ second phase supporting, thus, its rapid dissolution into the perovskite phase with increasing temperature, i.e., a dynamic liquid phase formation–dissolution process with low densification could be assumed for the first sintering step.

In the second sintering step, with increasing temperature the incongruent melting of the $SrCrO_4$ second phase is completed, passing the composition from solid + liquid to a region of liquid-only (ternary?),[22] the viscosity of the liquid generated during sintering will decrease, the pore-filling and elimination of pores with a rapid particle rearrangement and densification takes place, and the grain-coarsening process via solution–precipitation mechanism, if any, would be favored, see Figs. 5–7. Full densification was never achieved in the present experimental conditions, which can be attributed to (1) a continued weight loss as consequence of the phase transformations during the global sintering process (2) an insufficient amount of liquid for densification and (3) to the permanent volatilization of some small amount of CrO_3 due to its high vapor pressure. All of these factors negatively contribute to the densification process of the perovskite samples. Although Ownby[32] postulated that vapor transport during the early steps of sintering gave rise to a particle growth, decreasing the driving force for sintering, so inhibiting the densification. However, he also stated that a rapid vapor transport during the final sintering stage favored pore mobility and increased densification. On the basis of our experimental work in which a high heating-rate for sintering was used, we can argue that a simultaneous and complex process of phase transformation–liquid phase formation–particle rearrangement–chromium oxidation–rapid vapor transport led to a relatively high densification in the final sintering step.[33–35] It could be assumed that at low temperatures (first sintering-stage) complete liquid-phase wetting did not occurr and densification was delayed. At high temperatures (second sintering-stage) and with apparently a sufficient amount of liquid phase a rapid homogenization of the liquid took place as an effect of the large capillary forces from the wetting liquid, which dominates the sintering process at this stage.[35] The relatively high densification can be, thus, explained by a rapid rearrangement of solid perovskite particles in the presence of liquid, with a small grain growth. However, the no achievement of fully dense perovskite bodies allowed us to assume that the amount of formed liquid was not sufficient for both the grain-coarsening and full densification.

As above mentioned, B site doped LSCM samples showed an increase in TEC with increasing Mg^{2+} content. If it is taken into account that the ionic radius for the hexagonal coordination of oxygen of the Mg^{2+} ions (0.086 Å) substituted for Cr^{3+} (0.0755 Å) at the B site,[36] it follows an increase of both the lattice parameters and the volume of the unit cell, see Table 1. Although it would appears a contradiction, but the evolution to a higher crystal symmetry (distorted orthorhombic structure) also led to a decrease in the anisotropy and, as a consequence, the TEC will increases. According to our results, $La_{0.8}\ Sr_{0.2}Cr_{1-x}\ Mg_x\ O_3$ compositions in which $x \leqslant 15$ mol% would be useful as interconnector materials for SOFC devices. The higher TEC with increasing

Mg content can be explained by the increase of the average ionic radius of B-site metals in the perovskite structure during the thermal expansion measurements. Although preliminar experiments, which is not the scope of the present work, indicated that B site doping with Mg^{2+} decreased the electrical conductivity of the LSCM sintered samples, but the electrical conductivity level (several tens of S cm^{-1} at 900 °C) can be considered as acceptable for such an application. However, further development to know its thermal expansion behaviour in reducing atmospheres is required.

5. Conclusions

The polymerized complex solution synthesis method results in the formation of a chromate phase (La,Sr)(Cr,Mg) O_4 solid solution with the monoclinic structure of $a=0.7024$, $b=0.7251$, $c=0.6641$, and $\beta=104.39°$. Perovskite (La,Sr)(Cr,Mg) O_3 solid solution, with a SrO concentration of 20 mol% and MgO concentration $\leqslant$20 mol%, is formed at a temperature as low as 750 °C by the decomposition of the (La,Sr)(Cr,Mg) O_4 chromate phase. The obtained pervskite solid solution almost single phase had the orthorhombic structure with $a=0.5487$, $b=0.7770$, and $c=0.5483$ nm. The as prepared calcined powders, always accompanied by a small amount of a residual second phase ($SrCrO_4$), were highly sinterable leading to dense bodies (higher than 97% theoretical density) after sintering at 1550 °C for 6 h in air.

The global sintering takes place in a two-stage shrinkage process, the first one at about 1220 °C occurrs with the formation of a small amount of liquid phase in the beginning of the incongruent melting of the chromate phase ($SrCrO_4$), and the second one above 1420 °C takes place with the chromate phase melting completion accompanied by a rapid rearrangement of the perovskite particles in the liquid. After sintering, no second phases were detected in the samples prepared by the polymerized complex solution method indicating, thus, its character as a transient liquid phase.

Mg doping to $La_{0.8}Sr_{0.2}Cr\ O_3$ showed a thermal expansion behavior in air similar to that observed for YSZ electrolyte, when the Mg content was $\leqslant$15%. Therefore, $La_{0.8}Sr_{0.2}Cr_{0.9}Mg_{0.1}O_3$ and $La_{0.8}Sr_{0.2}Cr_{0.85}Mg_{0.15}O_3$ can be considered as good interconnect materials for SOFC with respect to thermal expansion.

Acknowledgements

The present work was supported by the Interministerial Commission of Science and Technology (CICYT) under Contract MAT 2000-0815.

References

1. Meadowcroft, D. B., Some properties and applications of strontium-doped rare-earth perovskites. In *Proceedings of the Conference on Sr Containing Compounds*, ed. T. J. Gray. National Research Council, Halifax, Nova Scotia, 1973, pp. 118–135.
2. Wirtz, G. P., Summary of Panel Sesion on Interconnection Materials. In *Proc. of the Workshop on High-Temperature SOFC*, ed. H. S. Isaacs, S. Srinivasan and I. L. Harry. Brookhaven National Laboratory, Upton, NY, 1977, pp. 30–32.
3. Sakai, N., Kawada, T., Yokokawa, H., Dokiya, M. and Iwata, T., Sinterability and electrical conductivity of calcium-doped lanthanum chromites. *J. Mater. Sci.*, 1990, **25**, 4531–4534.
4. Koc, R., Anderson, H. U., Howard, S. A. and Sparlin, D. M., Structural sintering and electrical properties of the perovskite type (La,Sr)(Cr,Mn)O_3. In *Proc. of the First International Symposium on SOFCs*, ed. S. C. Singhal. The Electrochem. Soc. Inc, Pennington, NJ, 1989, pp. 220–241.
5. Sakai, N., Kawada, T., Yokokawa, H., Dokiya, M. and Iwata, T., Thermal expansion of some chromium deficient lanthanum chromites. *Solid State Ionics*, 1990, **40/41**, 394.
6. Schafer, W. and Schmidberger, R., Ca and Sr-doped $LaCrO_3$: preparation, properties and high-temperature applications. In *High Tech Ceramics Elseviers Science Publishing*, ed. P. Vincenzini. B.V. Amsterdam, Netherlands, 1987, pp. 1737–1742.
7. Anderson, H. U., Fabrication and property control of $LaCrO_3$ based oxides. In *Processing of Crystalline Ceramics*, ed. H. Palmour III, R. F. Davis and T. M. Hare. Plenum Press, New York, 1978, pp. 469–477.
8. Tai, L. W. and Lessing, P. A., Modified resin-intermediate processing of perovskite powders. *J. Mat. Res.*, 1992, **7**(2), 502–519.
9. Kummar, S., Messing, G. L. and White, W. B., Metal organic resin derived barium titanate: I, formation of barium titanium oxycarbonate intermediate. *J. Am. Ceram. Soc.*, 1993, **76**, 617–624.
10. Duran, P., Capel, F., Tartaj, J. and Moure, C., Processing and charaterization of fine nickel oxide-dispersed zirconia-based composites prepared by polymeric complex solution synthesis. *J. Eur. Ceram. Soc.*, 2003, **23**, 2125–2133.
11. Manoharan, S. S. and Patil, K. C., Combustion synthesis of metal chromite powders. *J. Am. Ceram. Soc.*, 1992, **75**(4), 1012–1015.
12. Morelli, M. R. and Brook, R. J., Combustion synthesis of $LaCrO_3$ powders. In *Transations Ceramics, vol. 12, Ceramic Processing Science and Technology*, eds. G.L. Messing, H. Haussner and S. Hirano. 1996, pp. 81–85.
13. Kuscer, D., Ahmad-Khanlou, A., Hrovat, M., Holc, J., Bernik, S., Kolar, D., Naoumidis, A. and Tiez, F., Characterization of some perovskites as cathode materials for SOFC. In *Proc. of the Third Europ. SOFC Forum*, ed. P. Stevens (Nantes, France, 2–5 june). 1998, pp. 145–52.
14. Groupp, L. and Anderson, H. U., Densification of $La_{1-x}Sr_xCrO_3$. *J. Am. Ceram. Soc.*, 1976, **59**(9–10), 449–450.
15. Hayashi, S., Fukaya, K. and Saito, H., Sintering of lanthanum chromite doped with zinc or copper. *J. Mat. Sci. Lett.*, 1988, **7**, 457–458.
16. Milliken, C., Elangovan, S. and Khandkar, A., Interface reactions and sintering of doped $LaCrO_3$ materials. In *Proc. of the Intern. Symp. on SOFC (Nagoya, Japan, November 1989)*, ed. O. Yamamoto, M. Dokiya and H. Tagawa. Science House Co. Ltd, Tokyo, Japan, 1990, pp. 50–57.
17. Flandermeyer, B. K., Dusek, J. T., Blackburn, P. E., Dees, D. W., Macpheeters, C. C. and Poeppel, R. B., Interconnection development for monolithic SOFC, pp. 68–71 in Abstracts of 1986 Fuel Cell Seminar, Tucson, AZ, October, 1986.
18. Chen, C. C. and Anderson, H. U., Synthesis and characterization

of $(CeO_2)_{0.8}(SmO_{1.5})_{0.2}$ thin films from polymeric precursors. *J. Electrochem. Soc.*, 1993, **140**, 3555–3560.
19. Carter, J. D., Anderson, H. U. and Shumsky, M. G., Structure and phase transformation of lanthanum chromate. *J. Mat. Sci.*, 1996, **31**, 551–557.
20. Berg, R. W., Andersen, M. M. and Bjerrum, N. J., The crystal structure of $SrCrO_4$, a phase in $La_{0.8}Sr_{0.2}CrO_3$ samples, determined by Rietveld refinement of X-ray diffraction data. In *Proc. Riso Intern. Symp. on Material Science: High Temperature Electrochemistry Ceramics and metals*, ed. F. W. Poulsen, N. Bonanos, S. Linderoth, M. Mogensen and B. Zachau-Christiansen. Riso Nal. Laboratory, Roskilde, Denmark, 1996, pp. 175–180.
21. Mori, M., Hiei, Y. and Sammes, N. M., Sintering behavior and mechanism of Sr-lanthanum chromites with A-sites excess in air. *Solid State Ionics*, 1999, **123**, 103–111.
22. Negas, T. and Roth, R. S., The system strontium-chromium oxide in air and in oxygen. *J. Res. Natl. Bur. Stand., Sec. A*, 1969, **73**, 431–442.
23. Sakai, N., Kawada, T., Yokokawa, H., Dokiya, M. and Kojima, I., Liquid-phase- assisted sintering of calcium-doped lanthanum chromites. *J. Am. Ceram. Soc.*, 1993, **76**(3), 609–616.
24. Hiei, Y., Yamamoto, T., Itoh, H. and Mori, M., Controlling thermal expansion behaviour of Sr-doped lanthanum chromites with Al and Co for SOFC separators. *Proc. of the Third Europ SOFC Forum, Nantes, France*, 1998, 89–96.
25. Mori, M., Hiei, Y. and Sammes, N. M., Sintering behaviour of Ca- or Sr-lanthanum perovskites including second phase of $AECrO_4$ (AE = Sr,Ca) in air. *Solid State Ionics*, 2000, **135**, 743–748.
26. Mori, M., Enhancing effect on densification and thermal expansion compatibility for $La_{0.8}Sr_{0.2}Cr_{0.9}Ti_{0.1}O_3$-based SOFC interconnect with B-site doping. *J. Electrochem. Soc.*, 2002, **149**(7), A797–A803.
27. Mori, M., Application of designed perovskite oxides to the interconnect and cathode in SOFC, *Proc. of the fifth Europ. SOFC Forum*, Lucerne, Switherland, 2002, pp. 265–74.
28. Mori, M. and Sammes, N. M., Sintering and thermal expansion charaterization of Al and Co-doped lanthanum strontium chromites synthesized by the Pechini method. *Solid State Ionics*, 2002, **146**, 301–312.
29. Simmer, S. P., Hardy, J. S., Stevenson, J. W. and Amstrong, T. R., Sintering of lanthanum chromite using strontium vanadate. *Solid State Ionics*, 2000, **128**, 53–63.
30. Christie, G. M., Middleton, P. H. and Steele, B. C. H., Liquid phase sintering, electrical conductivity, and chemical stability of lanthanum chromite doped with calcium and nickel. *J. Eur. Ceram. Soc.*, 1994, **14**, 163–758.
31. Kingery, W. D., Bowen, H. K. and Uhlmann, D. R., *Introduction to Ceramics*, 2nd edn.. Wiley, New York, 1976.
32. Ownby, P. D., Oxidation state control of volatile species in sintering. *Mater. Sci. Res.*, 1973, **6**, 431–437.
33. Koc, R. and Anderson, H. U., Liquid phase sintering of $LaCrO_3$. *J. Europ. Ceram. Soc.*, 1992, **9**, 285–292.
34. Bates, J. L., Chick, L. A. and Weber, W. J., Synthesis, air sintering and properties of lanthanum and yttrium chromites and manganites. *Solid State Ionics*, 1992, **52**, 235–242.
35. Chick, L. A., Liu, J., Stevenson, J. W., Armstrong, T. R., Macready, D. E., Maupin, G. D., Coffey, G. W. and Coyle, C. A., Phase transitions and transient liquid-phase sintering in calcium-substituted lanthanum chromite. *J. Am. Ceram. Soc.*, 1997, **80**(8), 2109–2120.
36. Shannon, R. D. and Prewitt, C. T., Effective ionic radii in oxides and fluorides. *Acta Crystallogr.*, 1969, **B25**, 925–946.
37. Mori, M. and Hiei, Y., Thermal expansion behavior of titanium-doped $La(Sr)CrO_3$ so solid oxide fuel cell interconnects. *J. Am. Ceram. Soc.*, 2001, **84**, 2573–2578.